ISSN: 1992-8645 www.jatit.org E-ISSN: 1817-3195

SIMULATION OF GPR SCENARIOS USING FDTD

[1]GAMIL ALSHARAHI, [2]ABDELLAH DRIOUACH, [3]AHMED FAIZE

[1,2] Department of physic, Abdelmalek Essaâdi University, Faculty of sciences, Morocco

[3]Department of physic, Mohammed 1st University, Faculty polydisiplinarly, Morocco

E-mail : alsharahigamil@gmail.com, adriouach@hotmail.com, ahmedfaize6@hotmail.com

ABSTRACT

The Finite-Difference Time Domain (FDTD) method has become a standard simulation technique in computational electromagnetics. It has been extended and improved for accurately treating almost any kind of problem involving complex materials with arbitrary geometry and it continues to be an active field of research. The method has become so powerful that it is used as the computational core of not only many in-house tools but also commercial packages used to design electromagnetic systems (Reflexw, CST, EMPIRE, XFDTD, etc). Computational tools, such as FDTD, have become power-ful tools for GPR user, since the time-domain nature of FDTD-based programs enables the visualization of the causal evolution of complex electromagnetic phenomena such as the propagation of electromagnetic pulses in GPR scenarios that involve layered media, dispersive media, objects of arbitrary shape, etc. In the following paper several scenarios found during the GPR survey are simulated using FDTD and the results are commented on.

Keywords: *Ground Radar, Propagation, Electromagnetic Wave, FDTD Simulations.*

1. INTRODUCTION

The possibility of detecting buried objects, to localize the structures, and to determine the nature of the subsurface has always fascinated the word of research and engineering. However, there is no universal technique able to provide easy answers and accurate information on the geophysical component of the soil, as well as on their spatial distribution. The existing approaches include seismic methods, methods of electrical resistivity and induced polarization techniques generally referred to imaging of the near surface [5,6]. Ground penetrating Radar (GPR) is an interesting device that can allow a non-destructive auscultation [7] of the underground without any excavation. It is based on the use of high frequency electromagnetic waves, including reflection or diffraction that allows the detection of buried objects. Within the context of this work, we are interested in the use of an imaging method based on the propagation of electromagnetic waves emitted and recorded on a sensor. The GPR emits high frequency waves in the direction of the subsoil, whose ratings range from 10 MHz to 2.6 GHz. Detecting and / or location through the soil is highly needed in order to see the content of the soil without destruction or excavation. It will be, then, possible to draw diagrams of the subsoil and to locate searched objects.

The purpose of this section is to simulate the propagation of electromagnetic waves of GPR in the massive concrete and the ground that assumed heterogeneous environment and we will use antennas with different frequencies [3]. The propagation phenomenon will be studied through the reflected waves [9]: Working principle on which the GPR is based. For the treatment of data, Reflexw software will be used. A number of models will be designed to simulate a variety of geological conditions. In the first example, a rectangular bar of iron has been buried in the massive concrete. In the following examples, we consider a laminate, then a soil with a cavity inside. The radargrams associated with these different configurations will be given.

2. MEASUREMENT PRINCIPLES

Standard ground penetrating radar systems consist of a transmitting and a receiving antenna. High-frequency (range: 0.1 MHz to 2.6 GHz) electromagnetic pulses are emitted into the ground by the transmitting antenna (figure 1a). The radar wavelet propagates through the soil while the velocity of the wavelet depends on the dielectric properties of the ground as shown in Figure 1b. At interfaces, e.g., boundaries of different soil layers or distinct objects, where the dielectric properties of the different media change erratically, the electromagnetic wave is partially reflected. The

Journal of Theoretical and Applied Information Technology
31st August 2015. Vol.78. No.3

ISSN: 1992-8645 www.jatit.org E-ISSN: 1817-3195

travel time and amplitude of the wavelet is recorded by the receiving antenna [4].

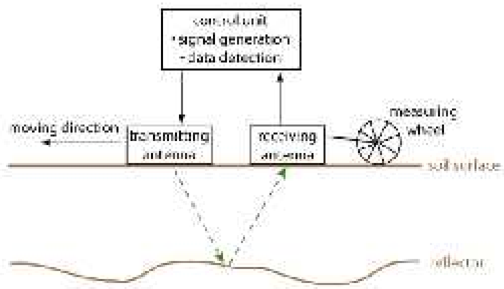

Figure 1a): Ground Penetrating Radar Measurement Principle [4]

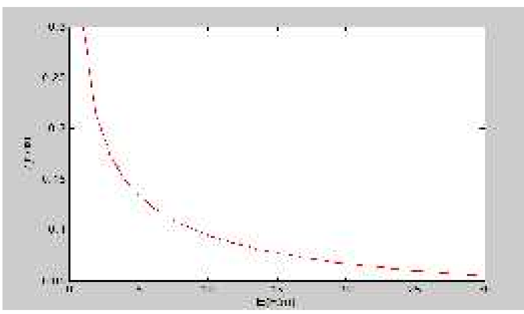

Figure 1b): Relationship Between Velocity And Dielectric Constant

3. DESCRIPTION MATERIALS AND SOFTWARE

3.1 Reflexw Software

Reflexw is software that is well suited for the treatment of data from various original seismic measurements, Georadar, ultrasound, this tool offers five analysis modules: Module 2D data-analysis, ModuleCMP velocity analysis, Module 3D data interpretation, Module modelling 2D-simulation, Module traveltime analysis 2D [2].

Figure 2: Reflexw Software [2]

The Reflexw software offers a diverse range of treatments:

a) 1D and 2D filters b) Migration

d) Gains (linear, exponential, local ...)

c) Interpolation

3.2 RADAN 7 software

RADAN 7 is The Most Advanced GPR Data Processing Software. RADAN 7 is GSSI state-of-the-art post-processing software. With its modular design, this program allows users to select the processing functions that best suit their professional needs. RADAN 7 is also Windows based, providing a familiar and easy-to-use environment for all levels of experience [8].

3.3 GPR (SIR System-3000Manual)

Like any measuring device, the GPR radar is characterized by its own performance. The maximum depth of investigation and resolution remain important technical parameters that guide the user. However, subsurface radar performance may be affected depending on the type of dielectric medium probed and the application. According to the application to which the GPR radar is designed, it will promote a maximum depth as an optimal resolution. Many comparative studies have been conducted to estimate the performance of various radar systems depending on the type of application for guiding the user in choosing the most appropriate system.

Figure 3: Gpr System-3000manual

3.4 Antennas

The radar offers a range of antennas operating at various frequencies. Among the working frequencies we find the following:

a) Shielded antennas: 100 MHz, 200 MHz, 400 MHz, 800 MHz, and 1.6 GHz

b) Unshielded antennas: 10 MHz, 20 MHz, 40 MHz, 100 MHz, 200 MHz

c) Drilling antennas: 100 MHz and 200 MHz.

Journal of Theoretical and Applied Information Technology
31st August 2015. Vol.78. No.3

ISSN: 1992-8645 www.jatit.org E-ISSN: 1817-3195

4. SIMULATION OF SIGNALS GEORADARS

Simulate signals GPR, Reflexw requires a number of parameters such as the frequency of the antenna used, the geometry of the ground, the dielectric permittivity, magnetic permeability and electrical conductivity of the media involved in the simulation.

4.1 Iron buried in a massive concrete

The massif is supposed to consist of a layer of 2.5 m in height over a length of 10 m wide. The massif in which the bar is buried dielectric accepts the following characteristics: ε_r=9 F/m and σ=0.01 S/m. The conductivity of iron bar σ=9.93 106 S/m and ε_r=1. 45 F/m [3], is buried at a depth of (1 m and 0.30 m) and is located between 4.50 m and 5.50 m in the horizontal direction, figure 5. The frequency simulation is set at 200, 400, 800 MHz. Each transmission and reflection of the simulated signal is recorded over a time window of 50 ns with a spatial increment of 0.025 m.

The results obtained are summarized and shown as radargram as shown in Figure 5. In this figure we see the presence of two diffraction hyperbolas which indicate the presence of the iron bar to around 0.5 m, that is to say exactly twice the depth to which the bar is buried.

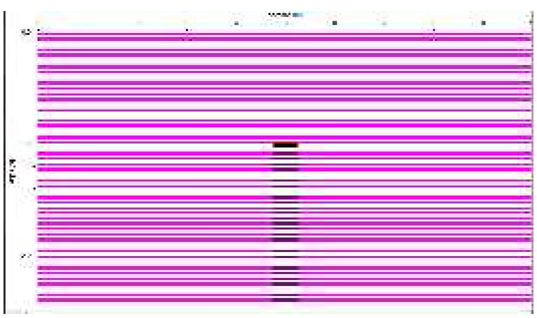

Figure 4: Diagram Representing The Position Of The Iron Bar In The Concrete Block

Figure 5a): Radargram Of The Buried Iron Bar In The Massive Concrete For The 200 Mhz Antenna.

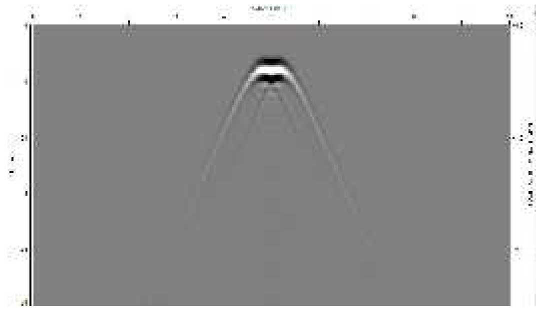

Figure 5b): Radargram Of The Buried Iron Bar In The Massive Concrete To The Antenna 400 Mhz And 0.30 M Deep.

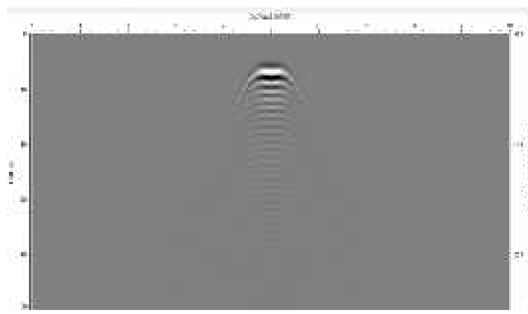

Figure 5c): Radargram Of The Buried Iron Bar In The Massive Concrete To The Antenna 800 Mhz And 0.30 M Deep.

Figure 5: Radargram Of The Buried Iron Bar In The Massive

4.2 Layered soil

The soil profile is that which admits a stratified three homogeneous layer to overlap. The depth is 1.5 m and we take a particle of length equal to 10 m. The electrical and magnetic characteristics of the layers are given in Table1. The frequency used is 200, 400, 800 MHz. The thicknesses of layers are: Dry sand layer 10 m x 0.50 m, limestone layer 10 m x 0.50 m, saturated sand layer 10 m x 0.50 m.

Table 1: Features Layers Up The Ground Modeled [3]

Material	Relative permittivity $\varepsilon_r(F/m)$	Conductivity $\sigma(S/m)$
Dry sand	7	0.00001
Limestone	5	0.002
Sandy saturated	30	0.001

ISSN: 1992-8645 www.jatit.org E-ISSN: 1817-3195

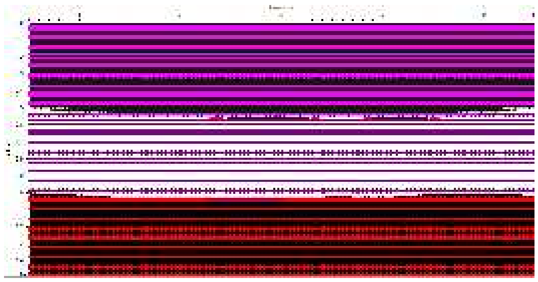

Diagram Showing The Position Of The Three-Layer

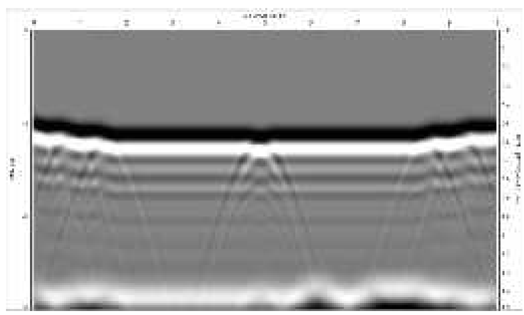

Figure 6a): Radargram Of The Sorting Sublayer For The 200 Mhz Antenna

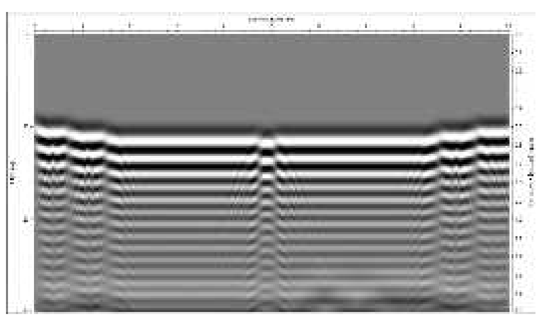

Figure 6b): Radargram Of The Sorting Sublayer For The 400 Mhz Antenna.

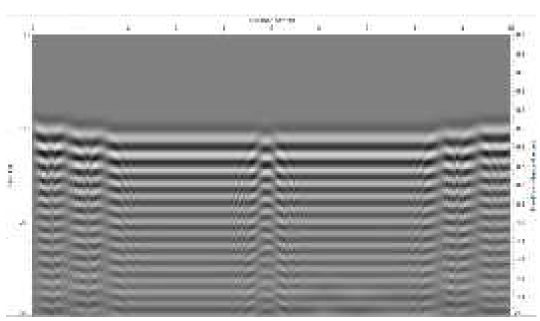

Figure 6c): Radargram Of The Sorting Sublayer For The 800 Mhz Antenna.

Figure 6: Radargram Of The Sorting Sublayer

The radargram of Figure 6 clearly distinguishes the three layers that make up the ground. Several inter-reflections are visible on this radargram.

4.3 Solid concrete having a cavity

This case is a massive concrete where a buried cavity. The radargram obtained differs depending on the material that fills this cavity. The goal is to see if we can identify the nature of the material by a simple examination radargram.

The massive length is 8 m and its depth is 2 m deep. It contains a circular cavity of 0.2 m in diameter at a depth of 1 m from the ground surface. The medium in which the cavity is buried admits the following dielectric characteristics shown in Table 2.

Table 2: Dielectric Properties Of Concrete With A Massive Problem Cavity [3]

Material	Relative permittivity ε_r(F/m)	Conductivity σ (S/m)
Concrete	6	0.015
Air	1	0
Clay	19	0.021
Dry sand	7	0.00001

The diagram of this structure is given by the Figure

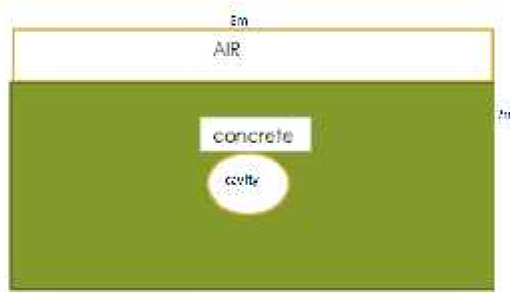

Concrete Massif Profile Containing A Cavity

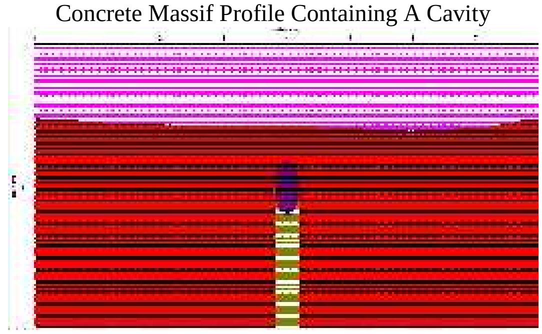

Diagram Showing The Position Of The Cavity

ISSN: 1992-8645 www.jatit.org E-ISSN: 1817-3195

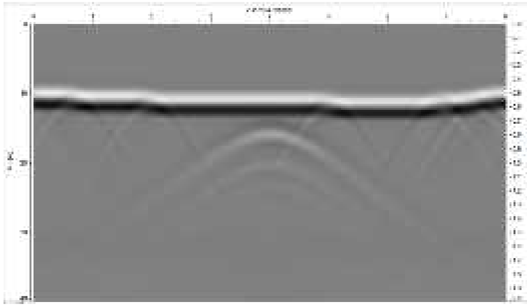

Figure 7a): Radargram Of The Model With Air-Filled Cavity For The 200 Mhz Antenna.

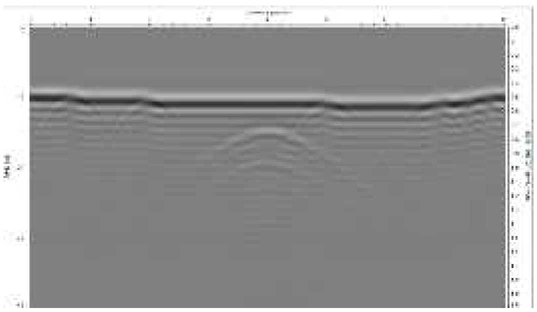

Figure 7b): Radargram Of The Model With Air-Filled Cavity For The 400 Mhz Antenna.

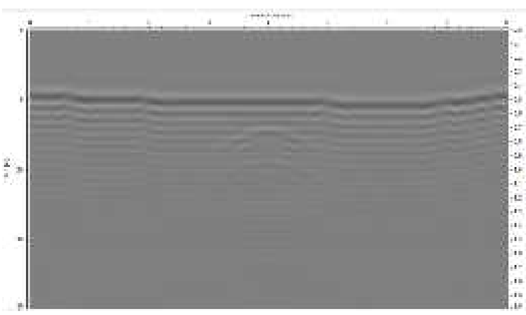

Figure 7c): Radargram Of Th Model With Air-Filled Cavity For The 800 Mhz Antenna.

Figure 7: Radargram Of The Model With Air-Filled Cavity

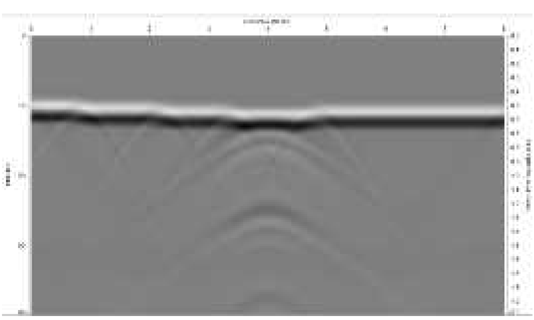

Figure 8a): Radargram Of The Model With Cavity Filled With Clay (200mhz)

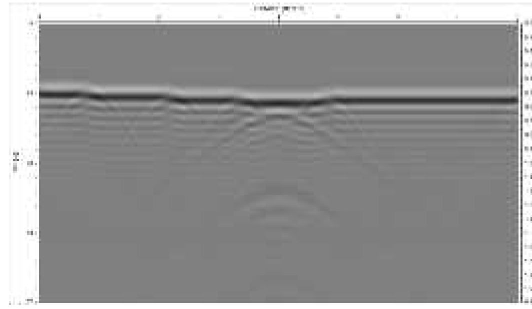

Figure 8b): Radargram Of The Model With Cavity Filled With Clay (400mhz)

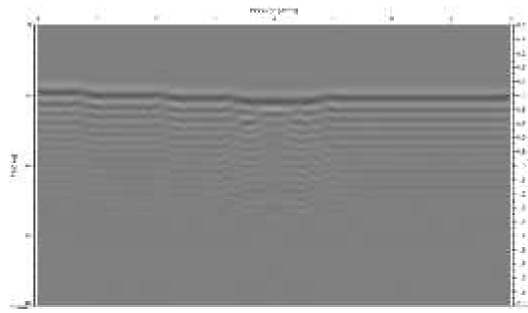

Figure 8c): Radargram Of The Model With Cavity Filled With Clay (800mhz)

Figure. 8: Radargram Of The Model With Cavity Filled With Clay

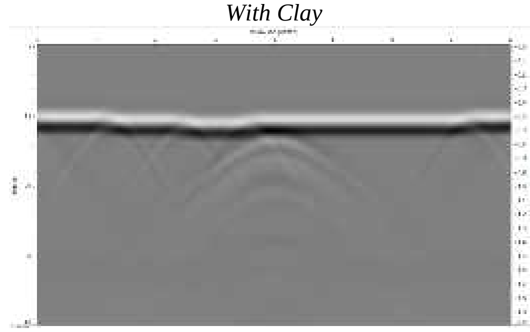

Figure 9a): Radargram Of The Model With Cavity Filled With Dry Sand (200MHZ)

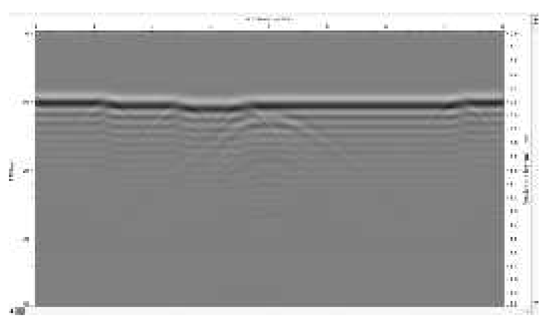

Figure 9b): Radargram Of The Model With Cavity Filled With Dry Sand (400mhz)

ISSN: 1992-8645 www.jatit.org E-ISSN: 1817-3195

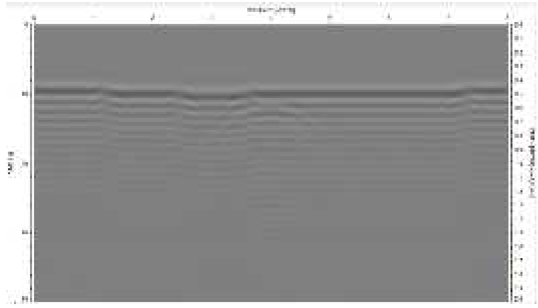

Figure 9c): Radargram Of The Model With Cavity Filled With Dry Sand (800mhz)
Figure 9: Radargram Of The Model With Cavity Filled With Dry Sand

Analysis of the radargrams given in figures 8 to 9 show that the location of the cavity is perfectly possible whatever the material that fills it. The contrast is better with dry sand and air and less good and moderate with clay. The structure of the reflections that appear under the main hyperbole can reveal the geometric shape of the cavity.

The problem of identification of the material filling the cavity is not easy since several combinations of material that may produce almost the same radargrammes. However, qualitative assessments can be drawn. Indeed the radargram of Figure 8 shows the existence of an environment with high permittivity and low dissipation. The radargrams of Figures 8 and 9 shows, on the contrary, environments with high dissipation or low permittivity. The inverse problem cannot be solved here easily without other information.

5. CONCLUSION

The dependence of the electromagnetic wave dielectric parameters of the propagation medium is the source of signal distortion, attenuation and dispersion during propagation and reflections that occur. In general, these mechanisms act on the waveform and on the visible contrast in the radargram in B-scan mode, for example. The simulations with different middle configurations allowed us to see that the permittivity manages the reflection of the wave while the conductivity governs the attenuation that develops in the middle. In addition the perfect permittivity of dielectric medium is greater when the amplitude of the reflected wave increases. Furthermore more diminish and vanish, for good conductors, it goes up to a total reflection. This dual effect of attenuation and reflection does not solve the inverse problem on identifying the nature of the heterogeneity met without other sources of information. In this work, the simulation of GPR scenarios using FDTD to help the interpretation of the data collected has proved to be very helpful.

REFRENCES:

[1] K. S. Yee (1966). Numerical solution of initial boundary value problems involving Maxwell. IEEE, Transaction Antennas and Propagation, 14: 302-307.

[2] K.J. Sandmeier (1998), Reflexw Version 4.5. Logiciel scientifique, Licence number 597 licenced to “centrotecnologicoDelMarmol y la PiedraSpainJ. Clerk Maxwell, A Treatise on Electricity and Magnetism, 3rd ed., vol. 2. Oxford: Clarendon, 1892, pp.68–73.

[3] Ground Penetrating Radar - 2n d Edition, Edite dbyDavidJ. Daniels

[4] Electromagnetic Methods in Applied Geophysics,Version: January 2011

[5] González García S., Rubio Bretones A., García Olmedo B. and Gómez Martín R. 2001. Time domain techniques in computation electromagnetics. Finite difference time domain methods.

[6] Harry M. Jol, „Ground Penetrating Radar: Theory and Applications‟. Elsevier Science. First edition 2009

[7] Reynolds, J. M., 1997. An Introduction to Applied and Environmental Geophysics. John Wiley & Sons, Chichester, England, 796 p.

[8] http://www.geophysical.com/software.htm

[9] Gurel, Levent and Ugur Oguz. 2001. Simulations of Ground Penetrating Radar over lossy and Heterogenous Grounds. IEEE Transaction Geosciences andRemote Sensing 39: 1190-1197.